International Journal for Multidisciplinary Research (IJFMR)
E-ISSN: 2582-2160 ● Website: www.ijfmr.com ● Email: editor@ijfmr.com

Enhancing the Electrical, Dielectric, and Structural Properties of CeO2-ZrO2 Nanocomposites

Imran Khan[1], Anis Ahmad[2]

[1]Department of Physics, Gandhi Faiz-E-Aam College Shahjahanpur, MJP Rohilkhand University Bareilly -242001, INDIA
[2]School of Basic Sciences (Physics), Galgotias University, Greater Noida -203201, INDIA

ABSTRACT

For enhancing the breakdown strength and increase the capacity of high voltage power supply with high oxidation stability and good electric properties, Ceramic nanomaterials like zirconia (ZrO_2) and Ceria (CeO_2) preferred due to their strong insulating property and high relative permittivity. In this article, we have reported the synthesis of CeO_2/ZrO_2 nanocomposite by chemical method. The use of surfactants during synthesis have an adverse effect on the catalytic activity of CeO_2 with different morphologies like nanorods, nanocubes, and nano-octahedra. In addition, zirconia can be synthesized via a variety of techniques, including sol-gel, hydrothermal, and precipitation procedures, and combined with other metal oxide nanoparticles. The synthesized nanocomposites were analyzed by X-ray diffraction (XRD), scanning electron microscope (SEM). The crystalline nature and mixed phase of CeO2/ZrO2 nanoparticles have been confirmed by the findings of XRD and SEM analysis. At various frequencies and temperatures, the dielectric constant and dielectric loss of the synthesized nanoparticles were determined. The conductivity and dielectric characteristics of the synthesized samples exhibited temperature and frequency dependency, indicating that the dopant concentration had a significant impact. As frequency increased, the nanoparticles' tangent loss and dielectric constant dropped sharply. These nano-composites can be used as a metal oxide semiconductor for memory devices as well as fuel cells.

Keywords: CeO_2/ZrO_2 nanocomposite, fuel cells, Conductivity, Dielectrics and Metals.

Introduction:

Nanostructures materials show very good refractory properties, chemical resistance, mechanical resistance and hardness both at normal and high temperatures. Ceria (CeO2) and Zirconia (ZrO2) nanoparticles are important material using in the composites for playing a prominent role in material science because their high strength, high fracture toughness, high hardness and good structural, chemical, electrical and dielectric properties. Nanocrystalline materials possess an interesting physical and chemical properties, which are different from their bulk counterparts, such as low density, smaller particles size, large surface area, stability, etc. Structural and electronic properties actually drive the physical and chemical properties of the solid and the effect of size is very much related to the electronic properties of the oxide [1-6]. In any material, the nanostructure produces the quantum dot effect or the confinement effects which essentially arise from the presence of discrete electronic states. Ceria also

helps in maintaining the dispersion and stability of the noble metals. We know that high dielectric materials (high-k) are considered as potential materials in the fabrication of electronic devices. There are different dielectric materials currently being used in metal oxide semiconductor field-effect transistors (MOSFETs), as gate oxide materials, as capacitor in memory devices and insulator in back-end interconnects. The silicon dioxide (SiO_2) is highly compatible with silicon technology and exhibits high interface quality. However, direct tunneling of charge carriers occurs via the potential wall as the SiO_2 layer thickness decreases, which in turn leads to increase in leakage current through gate dielectrics. For thin SiO_2 film, the leakage current from electron tunneling through the dielectrics is a problem [7-10]. Mahwish Bashir et al reported that Zirconium oxide (ZrO_2) prepared by Sol-gel method, enhanced functional or mechanical properties as well as purity, homogeneity and improved microstructure. It does not require vacuum and allow fabricating a large area with low cost and at low processing temperature.

The oxide nanoparticles are used to design energy efficient lithium ion batteries, light emitting diodes, solar cells, fuel cells and transistors, hydrogen storage devices, air purification, water purification, gas sensing, temperature and humidity sensing studies, drug delivery and bio imaging studies [11-20]. Thin ZrO2 films are also suitable dielectrics for volatile dynamic random access memory and for complementary metal-oxide-semiconductor devices [21-22]. Commonly, thin ZrO2 films are synthesized using electron beam physical vapor deposition [23], chemical vapor deposition [24] and atomic layer deposition [25].

High dielectric constant materials are uses in DRAM and MOS devices as a gate dielectrics and storage capacitors and as an ultra-large scale integrated circuits. Some of the dielectric materials like $SrTiO_3$, Ta_2O_5, Al_2O_3, ZrO_2, and HfO_2 consisting high gate capacitance, low leakage current, good thermal stability. ZrO2 has high dielectric constant nearly 25 with energy band gap from 4.6 to 7.8 eV and high permittivity [26]. The dielectric parameters were reported by Tokeer Ahmad et al. [27], with variation of frequency in a range from 20KHz to 1MHz at room temperature shows that the dielectric constant decreases with increase in frequency. On account of space polarization effect, the zirconia nanoparticle shows high dielectric constant at lower frequency region. However, at higher frequency region the polarization effect reduces which raises the decrease in dielectric constant. The dielectric characteristics of the nanocomposites were studied as a function of frequency and temperature. The room temperature dielectric constant and dielectric loss values were found to be 7.5 and 0.0094 for the synthesized nanoparticles at 500kHz. CeO_2-ZrO_2 nanoparticles can be used as resistive sensors and as a dielectric substance it used in dental treatment, fuel cell and as an electrochemical agent.

Experimental Procedure:

Zirconium oxychloride and sodium hydroxide (NaOH) chemicals were used for the production of the zirconium oxide nanoparticles. All analytical grade (AR) chemicals were used without further purification. The well-known Evaporation induced self-assembly (EISA) method was used for the synthesis of CeO_2–ZrO_2 nanocomposites. Porous CeO_2-ZrO_2 solid solutions were prepared through the EISA method. L. Almar et all. (28) reported that in a typical synthesis procedure, 10 mmol $Ce(NO)_2$ $6H_2O$ and $Zr(NO_3)_4$ $6H_2O$ with designed proportions were dissolved in 50 mL deionized water. About 0.1gm P123 and 0.1 mmol Polyvinyl pyrrolidone were dissolved into 100 mL ethanol. Subsequently, a transparent mixture was formed by directly mixing the two solvents. The solvent was placed in a beaker, and it was then covered with a thin layer of polyethylene with a few tiny pores. The solvents were then continuously evaporated at 60ºC until the raw solution was completely dried to form a solid precursor.

Then, the two solvents were mixed directly to form a transparent mixture. The solvent was kept in a beaker and then covered by a polyethylene thin film containing a few small holes, and then was sustained at 60ºC to evaporate the solvents until the raw solution was totally dried to form a solid precursor. Calcinations were conducted according to the following steps: firstly, the precursor was kept in a furnace at a heating rate of 2ºC/min to 200ºC and held for 1 hour to fully decompose the residual surfactants; then the temperature was elevated to 600ºC at a heating rate of 4ºC/min and kept for 4 h to obtain the as-prepared products.

Sigwadi et al (29) reported the preparation of zirconium oxide by hydrothermal method. According to him ZrO_2 nanoparticles were prepared by means of the hydrothermal method; $ZrOCl_2{\cdot}8H_2O$ and NaOH were used as starting materials. Zirconium hydroxide's precipitation ($Zr(OH)_4$) was obtained by slowly adding 5Ml NaOH to the aqueous solution of 0.5M $ZrOCl_2{\cdot}8H_2O$, at room temperature, while continuously stirring with a magnetic stirrer and mixed for 30min. The resulting solution was then transferred to an autoclave with a Teflon liner. The sample run was at a temperature of 120°C, with 400 rps and zero bar pressure for 48h. The resulting product was centrifuged and washed with distilled water until the pH was neutral. Then it was dried overnight at 80°C.

S. Usharani and V. Rajendran (30) prepared CeO_2/ZrO_2 nanocomposites by mixing of 0.1 M of cerrous chloride and zirconium oxy chloride octahydrate in water and stirred it for 30 min at room temperature to ensure the formation of the homogeneous mixed salt solution. Then cationic surfactant (CTAB) were added together and stirred for 1 h at room temperature. After the completion of 1 h the aqueous ammonium hydroxide solution was added drop-wise to attain the pH-6.5 and stirred continuously for 2 hrs. The resultant product was dried for 12 hrs. at 120^0C. After that, it was washed with water several times and then calcined at 600^0C for 8 hrs.

(a) Sample preparation:

Thin films of different thickness have been prepared by using pulsed laser deposition (PLD) technique, onto glass and silicon wafer substrates at different temperature on a base pressure of 10^{-8} Torr. The substrates were thoroughly cleaned in a detergent solution and then in a chromic acid and finally, cleaned using trichloroethylene. Double distilled water was used throughout in different stages of cleaning. To avoid the fractionation of the alloy during evaporation and, thereby, to ensure the correct average composition of the films formed, a high deposition rate was used to prepare the studied films. The thickness of the films was measured by using a quartz crystal monitor.

(b) Structural study and microscopic measurements:

To understand the behavior of a crystal we have to study the structural properties of materials. So XRD will be used to verify the crystallinity and the structure of these as grown nanostructures. For Rietveld refinement in the crystalline state, the data will be fitted using FULLPROF code. The detailed microscopic studies have been carried out using Scanning Electron Microscope (SEM).

(c) Electrical transport measurements:

Investigations on the temperature dependence of conductivity, the effect of impurities on activation energy, the effect of annealing on conduction and the effect of high electric field on conduction mechanism is a subject of great importance because the results of such studies provide ways to control conductivity effectively. The density of localized states in the mobility gap controls many physical properties of amorphous semiconductors. The determination of density of states near the Fermi level N (EF) has been an important issue in these materials. One of the direct methods for the determination of N (EF) involves the measurement of space charge limited conduction (SCLC) which can be easily

observed in low conductivity semiconducting materials. The electrical transport properties of these nanostructures materials will be studied in the temperature range from room temperature to 500K. For that we used ohmic contact method to measure I-V characteristics at different temperature and R-T characteristics to explain the transport mechanism.

(d) Dielectric properties measurements:

A specially designed metallic sample holder is used for DC as well as AC measurements. The sample holder consists of two parts; the upper part contains two steel electrodes passes through Teflon feed, between which the samples were mounted via a screw arrangement. The lower part contains a heating element in the bottom to heat the sample. For both DC and AC measurements, the vacuum of the order 10^{-3} torr maintained inside the sample holder. The temperature was measured by mounting a k-type Chromel-Alumel thermocouple near the sample. A Keithley picoammeter (model 6485) was used to measure the currents between temperatures from room temperature to 500^0K. For dielectric properties, the capacitance C and dissipation factor D is measured by using Wayne Kerr 4300 LCR meter (frequency range 20 Hz-1 MHz with 0.1% basic accuracy).

Result and Discussion:

Structural Characterization:

In fig-1, the microstructure of the powdered samples is shown in the SEM images of fractured surface of the samples. The volume of pores and grain size can be seen clearly.

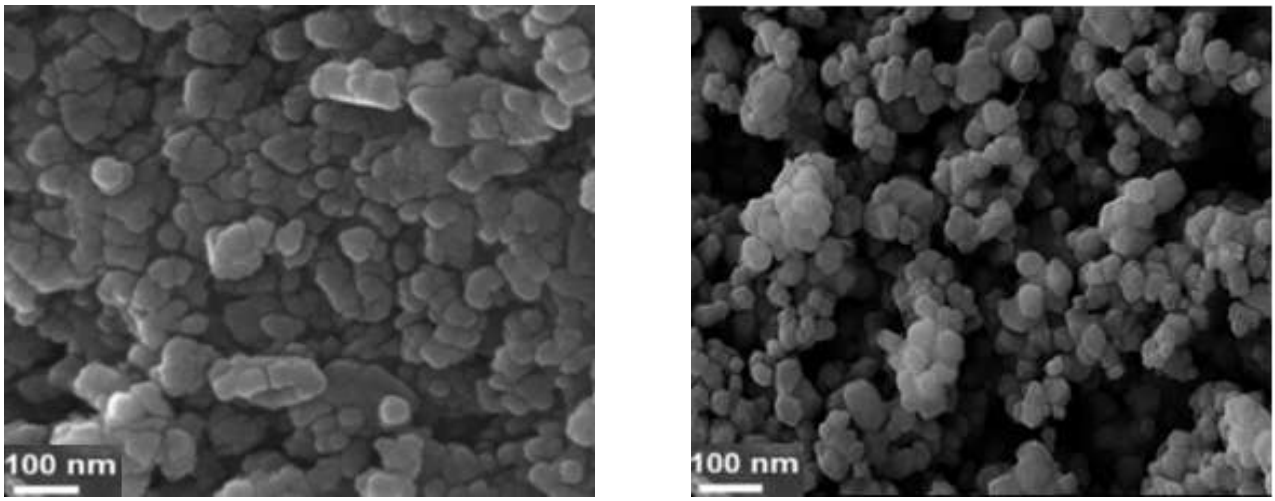

Fig.1: SEM images of CeO_2-ZrO_2 nanocomposite.

The surface of this particular elongated grain shows distinct evidence of crack growth along the surface of the grain. Such a growth mode helps to produce a complex crack path, which in turn contributes to crack deflection and bridging, thereby improving the toughness of these samples. The SEM image shows the dispersed spherical morphologies.

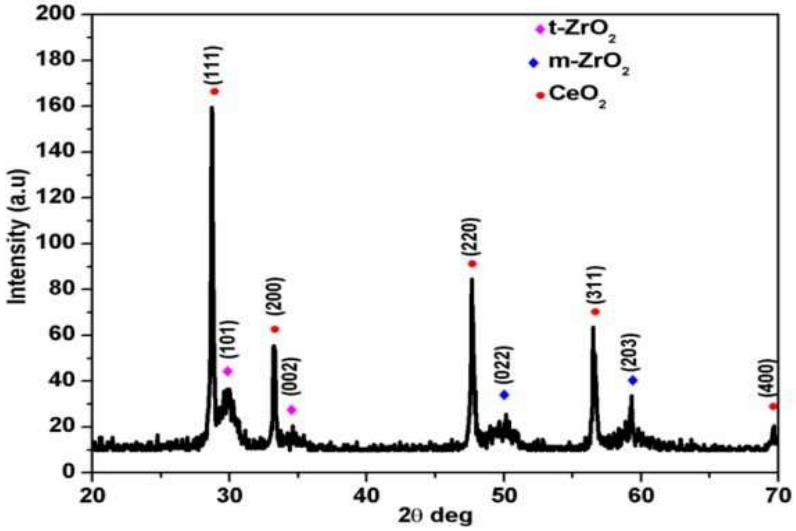

Fig.2: XRD pattern of CeO_2-ZrO_2 nanocomposite.

In fig-2 The X-ray diffraction pattern of CeO_2-ZrO_2 nanocomposites are shown. The four peaks in the pattern with 2θ values of 29.8, 34.4, 49.6 and 59.1 correspond to the (101), (002), (022) and (203) planes which indicates the formation of tetragonal and monoclinic structure of ZrO_2 and Similarly, the five peaks with 2θ values 28.6, 33.2, 47.6, 56.4 and 69.6 that are correspond to the (111), (200), (220), (311) and (400) planes that indicates the formation of pure phase CeO_2.

Electrical transport measurements:

For electrical characterization of the material impedance and interfaces present in these materials. The impedance measurements data gives both resistive (real) and reactive (imaginary) components for a material.Fig.3 presents the variation of a.c conductivity with frequency for pure and Zr-doped CeO2 samples The conductivity with frequency rang 500 hz to 50 Khz are shown as increasing trend on the basis of electron hopping from one site to another. The mobility of charge carriers plays an important role in the variation of conductivity of these heterogeneous materials. Zr4+ ions replace the Ce4+ ions in these structures and hopping with the addition of oxygen ions. This type of hopping becomes more prominent at higher frequencies and thereby increasing the conductivity of Zr substituted compositions [31].

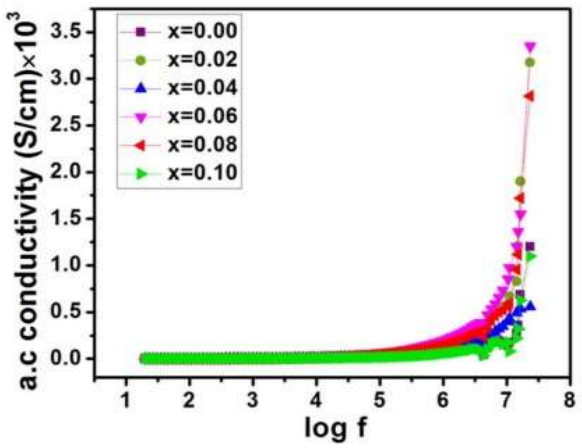

Fig.3 The variation of a.c conductivity with frequency.

Dielectric properties measurements:

The complex dielectric constant of a material consists imaginary (ε'') and a real part (ε').

$\varepsilon'' = \varepsilon' \tan\delta$ and $\varepsilon' = Cd/\varepsilon_0 A$

where C, d, A, ε_0 and tan δ represent capacitance, thickness, area of the sample, permittivity of free space, and dielectric loss respectively.

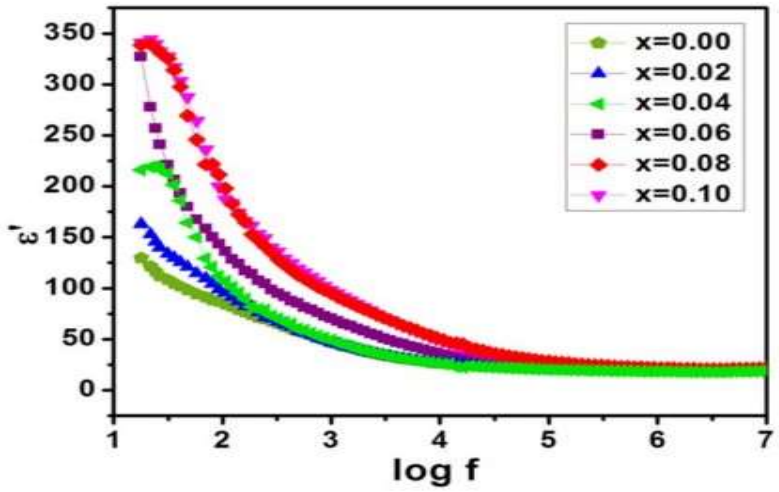

Fig.4 The variation of dielectric constant with applied frequency

The Dielectric constant (ε′) and dielectric loss (ε″) at different frequencies (100Hz to 1 MHz). The values of ε′ and ε″ from room temperature to (> 625K) remain almost independent of temperature. As the temperature are increases, ε′and ε″ increase quite appreciably with temperature. As we know the high dielectric constant materials are used in integrated circuits devices as a gate dielectrics and storage capacitors. Some of the dielectric materials like Zro2 and Ceo2 consisting high gate capacitance, low leakage current, good thermal stability. Here in fig-4 we have discussed sintered CeO2 samples in the form of a pallets for the dielectric measurements in the frequency range 100 Hz to 5 MHz [31]. The variation of dielectric constant and loss factor with applied frequency of sintered pellet of CeO2 is shown in Fig. 5.

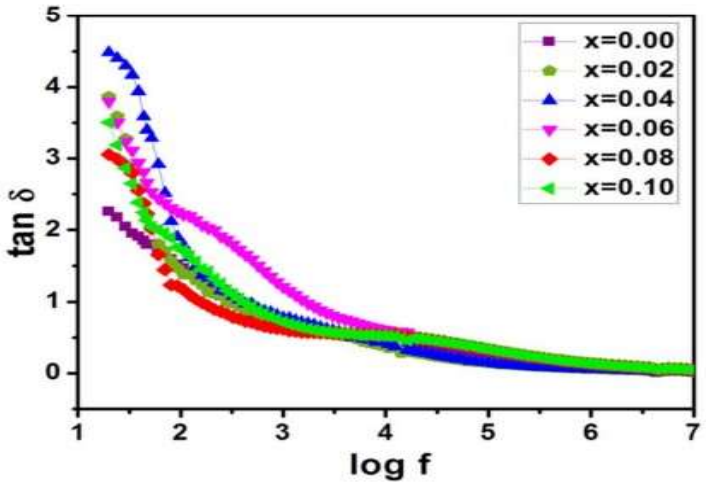

Fig.5 The variation of dielectric constant with applied frequency

So we can say that the collection of charges at their respective boundaries and the polarization value is subjected to increase [31-33]. Furthermore, decreasing trend of ε′ with increasing frequency can be explained on the basis of Maxwell-Wagner polarization mechanism which described that space charge polarization provide a prominent contribution at low frequencies but at higher frequencies orientational polarization is observed. This type of polarization produces as the frequency increasing the charge carriers find it difficult to cope with the changing electric field direction and thus the polarization decreases and so does the ε′ [34]. A similar trend is observed here for tan δ as compared with the ε′ plot in figure 5. The values of tan δ are observed as high at low frequencies which eventually decreases as the increase in frequency. The reason for high values of tan δ at low frequency is associated with the movement of dipoles with external applied electric field undergo rapid variation in their directions which causes an energy loss. As the frequency increases the dipoles do not follow the electric field variation and hence energy losses as well as tan δ values decrease subsequently [35]. The tan δ values are comparatively much smaller attributed to the low losses in the presence of an electric field.

Conclusion:

The values of dielectric constants , ε′and ε″ rise significantly when the temperature rises. High dielectric constant materials are well-known for their application as storage capacitors and gate dielectrics in integrated circuits. The increase in conductivity throughout the frequency range of 500 Hz to 50 KHz is attributed to electron hopping between different sites. These heterogeneous materials' varying conductivities are significantly influenced by the mobility of charge carriers. As we know the high dielectric constant materials are commonly utilized in integrated circuit devices for storage capacitors and gate dielectrics. The values of tanδ has higher values at low frequencies and gradually decreases with increasing frequency. Energy losses and tanδ values decreases as a result of the dipoles' inability to follow variations in the electric field as the frequency rises. Carbonitrides and nitrides were produced in the past 5 years by selective etching and exfoliation of layered ternary precursors forming a large family of 2D materials named MXenes. In addition of the composition, the electrical conductivity of MXenes depends on the sample preparation method. for high-performance, high rate batteries. MXenes provide a conductive matrix that accommodates expansion and contraction of particles while maintaining structural and electrical connectivity. Other applications have also been studied such as water purification, reinforcement for composites, electro catalysts and catalysts in the chemical industry, lubricants, photo catalysts, bio- and gas sensors.

References:

1. Tatiana. M. Arantes., et al “Stable Colloidal Suspensions of Nanostructured Zirconium Oxide synthesized by Hydrothermal Process. J. Nanopart. Res (2010).
2. Padma. Nimare., A. A. Koser. “Biological Synthesis of ZrO2 Nanoparticle using Azadirachta Indica Leaf Extract. IRJET Vol.3 Issue: 07 July 2016.
3. K. Geethalakshmi., T. Prabhakaran., J. Hemalatha. “Dielectric Studies on Nano Zirconium Dioxide Synthesized through Co-Precipitation Process.” Intl. J. of Mater. & Metallurgical Engineering. Vol. 6, No. 4, 2012.
4. Xinmei. Liu., Gaoqing. Lu., Zifeng. Yan. “Preliminary synthesis and characterization of mesoporous nanocrystalline zirconia.” Journal of Natural Gas Chemistry, Vol. 12, No. 3, 2003.

5. A.K. Singh., Umesh. T. Nakate. "Microwave Synthesis, Characterization and Photoluminescence Properties of Nanocrystalline Zirconia". The Scientific World Journal, Vol. (349457), 2014, 7.
6. R. Madhusudhana., M.A. Sangamesha., R. Gopal. Krishne. Urs., L. Krishnamurthy., G.L. Shekar. "Synthesis and Characterization of Zirconia by Simple Sol-Gel Route." International Journal of Advanced Research (2014), Volume 2, Issue 4, 433-436.
7. D. Rathee, M. Kumar and S.K. Arya, CMOS Development and Optimization, Scaling Issue and Replacement with High-k Material for Future Microelectronics Int. J. Comp. Appl. 8, 10-17 (2010).
8. S. Guha and V. Narayanan, Annu. *High-κ/Metal Gate Science and Technology*, Rev. Mater. Res. 39, 181-202 (2009)
9. A. Kingon, J.P. Maria, S.K. Streiffer, Alternative dielectrics to silicon dioxide for memory and logic devices Nature 406, 1032-1038 (2000)
10. Jung-Ho Yoo *et al*, A study on the microstructure and electrical properties of CeO2 thin films for gate dielectric applications , Microelectronic Engineering 56, 187–190 (2001).
11. Snaith HJ, Mende LS. Advances in liquid-electrolyte and solid-state dye-sensitized solar cells Adv Mater. 2007;19(20):3187–3200.
12. Gratzel M. Photo electrochemical cells. Nature. 2001; 414:338–344.
13. Asamoto M, Miyake S, Sugihara K, et al. Improvement of Ni/SDC anode by alkaline earth metal oxide addition for direct methane–solid oxide fuel cells, Electrochemistry Communications. 2009;11(7):1508, 1511.
14. Mamak M, Coombs N, Ozin G. Self-assembling solid oxide fuel cell materials: Mesoporous yttria-zirconia and metal-yttria-zirconia solid solutions, Journal of the American Chemical Society. 2000;122(37):8932– 8939.
15. 15. Sun B, Sirringhaus H, Solution-processed zinc oxide field-effect transistors based on self-assembly of colloidal nanorods, Nano Lett. 2005;5(12):2408–2413.
16. 16.Norris BJ, Anderson J, Wager JF, et al. Spin-coated zinc oxide transparent transistors, Journal of Physics D: Applied Physics. 2003;36(20):105– 107.
17. 17. Hepel M, Hazelton S. Nanomaterials and Energy Storage in a Glance: a Review, Electochim Acta. 2005;50(25– 26):5278–5291.
18. 18. Rout CS, Hegde M, Govindaraj A, et al. Ammonia sensors based on metal oxide nanostructures, Nanotech. 2007;18(20):205504(1–9).
19. 19. Zhao S, Wei P, Chen S. Enhancement of trimethylamine sensitivity of MOCVD-SnO2 thin film gas sensor by thorium, Chemical. 2000;62(2):117–120.
20. 20. Bae S, Lee SW, Takemura Y. Applications of NiFe2O4 nanoparticles for a hyperthermia agent in biomedicine, Appl Phys Lett. 2006;89(25):252503.
21. 21. PANDA, D. and TSENG, T. Y. Growth, dielectric properties, and memory device applications of ZrO2 thin films. Thin Solid Films. 2013, vol. 531, pp. 1-20.
22. 22. FIORENTINI, V. and GULLERI, G. Theoretical evaluation of zirconia and hafnia as gate oxides for Si microelectronics. Physical review letters. 2002, vol. 89, no. 26, p. 266101.
23. 23. SCHULZ, U. and SCHMÜCKER, M. Microstructure of ZrO2 thermal barrier coatings applied by EB-PVD. Materials Science and Engineering: A. 2000, vol. 276, no. 1-3, pp.1-8.
24. 24. CHANG, J. P., LIN, Y. S. and CHU, K. Rapid thermal chemical vapor deposition of zirconium oxide for metal-oxide-semiconductor field effect transistor application. Journal of Vacuum Science

& Technology B: Microelectronics and Nanometer Structures Processing, Measurement, and Phenomena. 2001, vol. 19, no. 5, pp.1782-1787.

25. 25. PERKINS, C. M., TRIPLETT, B. B., MCINTYRE, P. C., SARASWAT, K. C., HAUKKA, S. and TUOMINEN, M. Electrical and materials properties of ZrO2 gate dielectrics grown by atomic layer chemical vapor deposition. Applied Physics Letters. 2001, vol. 78, no. 16, pp. 2357-2359.
26. 26. Wang J, Zhao L, Luu N H, Wang D & Nakashima H, Structural and electrical properties of Zr oxide film for high-k gate dielectrics by using electron cyclotron resonance plasma sputtering. Appl Phys A, 80 (2005) 1781.
27. 27. Ahmad T, Shahazad M, Phul R. Dielectric, optical and enhanced photocatalytic properties of CuCrO2 nanoparticles Material Sci & Eng Int J. 2017;1(3):100–104.
28. 28. L. Almar, A. Morata, M. Torrell, M. Gong, M. Liu, T. Andreu, A. Tarancon., J. Mater. Chem. A 4(20) (2016) 7650-7657.
29. 29. Sigwadi et al. Preparation of a high surface area zirconium oxide for fuel cell application International Journal of Mechanical and Materials Engineering, (2019)14:5,1-11.
30. 30. S. Usharani and V. Rajendran, International Journal of Pure and Applied Physics, (12), No.1 (2016),53-60.
31. 31. Kumar M J K and Kalathi J T 2018 Low-temperature sonochemical synthesis of high dielectric lanthanum doped cerium oxide nanopowderJ. Alloy. Compd. 748 348–54
32. 32. Wang J, Zhao L, Luu N H, Wang D & Nakashima H, Structural and electrical properties of Zr oxide film for high-k gate dielectrics by using electron cyclotron resonance plasma sputtering Appl Phys A, 80 (2005) 1781.
33. 33. M Zafaret al Structural, dielectric and optical investigations of Zr incorporated ceria nanoparticles Mater. Res. Express 6 (2019) 116321
34. 34. Abbas S K, Atiq S, Riaz S, Ramay S M and Naseem S 2017 Thermally assisted electro-active regions in SrMnO3 ceramics Mater. Chem. Phys. 200 128–35
35. 35. Abbas S K, Aslam M A, Amir M, Atiq S, Ahmed Z, Siddiqi S A and Naseem S 2017 Electrical impedance functionality and spin orientation transformation of nanostructured Sr-substituted BaMnO3 hexagonal perovskitesJ. Alloy. Compd. 712 720–31